Inorg. Chem. **2008**, *47*, 7734−7744

A New Bis(1-naphthylimino)acenaphthene Compound and Its Pd(II) and Zn(II) Complexes: Synthesis, Characterization, Solid-State Structures and Density Functional Theory Studies on the syn and anti Isomers

Vitor Rosa,[†] Teresa Avilés,*[,†] Gabriel Aullon,[‡] Berta Covelo,[§] and Carlos Lodeiro[†]

REQUIMTE, Departamento de Química, Faculdade de Ciências e Tecnología, Universidade Nova de Lisboa, Caparica, 2829-516, Portugal, Departament de Química Inorgànica and Institut de Química Teòrica i Computacional, Universitat de Barcelona, Barcelona, Spain, and Unidad de Determinación Estructural, Proteómica y Genómica, CACTI Universidad de Vigo, 36310-Vigo, Spain

Received April 30, 2008

A new rigid bidentate ligand, bis(1-naphthylimino)acenaphthene, **L1**, and its Zn(II) and Pd(II) complexes [$ZnCl_2$(**L1**)], **1**, and [$PdCl_2$(**L1**)], **2**, were synthesized. **L1** was prepared by the "template method", reacting 1-naphthyl amine and acenaphthenequinone in the presence of $ZnCl_2$, giving **1**, which was further demetallated. Reaction of 1-naphthyl amine with acenaphthenequinone and $PdCl_2$ afforded dichloride bis(1-naphthyl)acenaphthenequinonediimine palladium, **2**. **L1**, **1**, and **2** were obtained as a mixture of syn and anti isomers. Compound **2** was also obtained by the reaction of $PdCl_2$ activated by refluxing it in acetonitrile followed by the addition of **L1**; by this route also a mixture of syn and anti isomers was obtained, but at a different rate. The solid-state structures of **L1** and the anti isomer of compound **2** have been determined by single-crystal X-ray diffraction. All compounds have been characterized by elemental analyses; matrix-assisted laser desorption ionization−time-of-flight−mass spectrometry; IR; UV−vis; ^{1}H, ^{13}C, and ^{1}H−^{1}H correlation spectroscopy; ^{1}H−^{13}C heteronuclear single quantum coherence; ^{1}H−^{13}C heteronuclear single quantum coherence−total correlation spectroscopy; and ^{1}H−^{1}H nuclear Overhauser effect spectrometry NMR spectroscopies when applied. Density functional theory studies showed that both conformers for [$PdCl_2$(BIAN)] are isoenergetic, and they can both be obtained experimentally. However, we can predict that the isomerization process is not available in a square-planar complex, but it is possible for the free ligand. The molecular geometry is very similar in both isomers, and only different orientations for naphthyl groups can be expected.

Introduction

α-Diimine ligands have been known for a long time[1,2] and are well-known to stabilize organometallic complexes.[3] They are derived from the condensation reaction of a diketone with two equivalents of an alkyl or arylamine often catalyzed by a Lewis or Brönsted acid. Using these synthetic routes, we can easily vary the backbone and the aryl substituent, thus enabling modification of the steric and electronic effects at the metal center. More recently, Elsevier et al.[4] described the synthesis and full characterization of the rigidly chelating bidentate nitrogen ligands (Ar-BIAN = bis(aryl)acenaphthenequinonediimine) by condensation of the rigid acenaphthenquinone with a proper amine. Palladium complexes with Ar-BIAN ligands were shown to be efficient catalysts for the homogeneous hydrogenation of electron-

* Author to whom correspondence should be addressed. Fax: +351-21-2948550. E-mail: tap@dq.fct.unl.pt.
[†] Universidade Nova de Lisboa.
[‡] Departament de Química Inorgànica and Institut de Química Teòrica i Computacional.
[§] CACTI Universidad de Vigo.

(1) (a) Dvolaitzky, M. *Acad. Sci. Paris, Ser. C* **1969**, *268*, 1811. (b) Dvolaitzky, M. *Chem. Abstr.* **1969**, *71*, 61566b.
(2) (a) Matei, I.; Lixandru, T. *Bull. Ist. Politeh. Iasi* **1967**, *13*, 245. (b) Matei, I.; Lixandru, T. *Chem. Abstr.* **1969**, *70*, 3623m.
(3) (a) Tom Dieck, H.; Svoboda, M.; Grieser, T. *Z. Naturforsch.* **1981**, *36b*, 832. (b) van Koten, G.; Vrieze, K. *Adv. Organomet. Chem.* **1982**, *21*, 151, and references cited therein. (c) Rosa, V.; Carabineiro, S. A.; Aviles, T.; Gomes, P. T.; Welter, R.; Campos, J. M.; Ribeiro, M. R. *J. Organomet. Chem.* **2008**, *693* (4), 769–775.
(4) van Asselt, R.; Elsevier, C. J.; Smeets, J. J. W.; Spek, A. L.; Benedix, R. *Recl. Trav. Chim. Pays-Bas.* **1994**, *113*, 88–98.

10.1021/ic800790u CCC: $40.75
Published on Web 08/01/2008

poor alkenes and carbon−carbon cross-coupling reactions[5] and for the selective hydrogenation of alkynes to alkenes.[6] A large number of late transition metal complexes bearing α-diimine ligands have been extensively employed in several other catalytic reactions.[7] We will recall among others the commercial production of polyolefins from ethene and propene,[8] and alkene−CO copolymerization.[9,10] The synthesis of atactic polyketones catalyzed by Pd complexes with meta-substituted Ar-BIAN ligands has been recently reported.[11] Oligomerization of ethylene using modified α-diimine ligands has been reported.[12] Ar-BIAN ligands with strong electron-withdrawing substituents on the aryl rings or mixed Ar,Ar′-BIAN having different substituents on the two aryl rings have been synthesized and their relative binding strengths studied.[13] The reactivity of these ligands with main group metals calcium and magnesium and metalloid germanium has also been studied.[14]

We report herein the synthesis and characterization of a new ligand: bis(1-naphthylimino)acenaphthene, **L1**, and its Zn(II) and Pd(II) complexes [$ZnCl_2$(**L1**)], **1**, and [$PdCl_2$(**L1**)], **2**. In **L1**, **1**, and **2**, syn and anti isomers are possible. The solid-state structures of **L1** and the anti isomer of compound **2** have been determined by single-crystal X-ray diffraction. All complexes have been characterized by elemental analyses; matrix-assisted laser desorption ionization−time-of-flight−mass spectrometry (MALDI-TOF-MS); IR; UV−vis; ^{1}H, ^{13}C, and ^{1}H−^{1}H correlation spectroscopy (COSY); ^{1}H−^{13}C heteronuclear single quantum coherence (HSQC); ^{1}H−^{13}C heteronuclear single quantum coherence−total correlation spectroscopy (HSQC-TOCSY); and ^{1}H−^{1}H nuclear Overhauser effect spectrometry (NOESY) NMR spectroscopy when applied. Density functional theory (DFT) studies showed that both conformers of [$PdCl_2$(BIAN)] are isoenergetic, and they can both be obtained experimentally. However, we can predict that the isomerization process is not available in a square-planar complex, but it is possible for the free ligand. The molecular geometry is very similar in both isomers, and different orientations only for naphthyl groups can be expected.

Experimental Section

General Procedures and Materials. All reactions were performed in the air, except the cases performed in an argon atmosphere using Shlenk techniques, as referred to in this section. Solvents were reagent grade and were dried according to literature methods. Elemental analyses were performed by Analytical Services of the Laboratory of REQUIMTE−Departamento de Química, Universidade Nova de Lisboa, on a Thermo Finnigan-CE Flash-EA 1112-CHNS instrument. Infrared spectra were recorded as Nujol mulls on NaCl plates using a Mattson Satellite FTIR spectrometer. NMR spectra were recorded using a Bruker AVANCE II 400 and 600 MHz device using the program TOPSPIN 2.0 (Bruker).

X-Ray Crystal Structure Determinations. Crystallographic data were collected on a Bruker Smart 1000 charged-coupled device diffractometer at CACTI (Universidade de Vigo) at 293 K using graphite monochromated Mo Kα radiation ($\lambda = 0.71073$ Å) and were corrected for Lorentz and polarization effects. The software SMART[15] was used for collecting frames of data, indexing reflections, and the determination of lattice parameters, and SAINT[15] was used for the integration of intensity of reflections and scaling. The data of **2** were corrected for absorption using the program SADABS.[16] The structures were solved by direct methods using the program SHELXS97.[17] All non-hydrogen atoms were refined with anisotropic thermal parameters by full-matrix least-squares calculations on F^2 using the program SHELXL97.[17] Hydrogen atoms were inserted at calculated positions and constrained with isotropic thermal parameters. Drawings were produced with PLATON[18] and MERCURY.[19] Special computations for the crystal structure discussions were carried out with PLATON.[18] Crystal data and structure refinement parameters are summarized in Table 1. The structural data have been deposited with the Cambridge Crystallographic Data Centre under reference numbers 671032 and 671033 for **L1** and **2**, respectively. The data can be obtained free of charge via www.ccdc.cam.uk/data_request/cif, by e-mailing data_request@ccdc.cam.ac.uk, or by contacting The Cambridge Crystallographic Data Centre, 12 Union Road, Cambridge CB2 1EZ, United Kingdom.

Spectrophotometric Measurements. Absorption spectra were recorded on a Perkin-Elmer Lambda 35 spectrophotometer. The linearity of the absorption versus concentration was checked in the concentration range used (1.0×10^{-4} to 1.0×10^{-6} M). All spectrophotorimetric titrations were performed as follows: the stock solutions of the ligand (*ca.* 1.0×10^{-3} M) were prepared by dissolving an appropriate amount of the ligand in a 50 mL volumetric flask and diluting it to the mark with freshly dry CH_2Cl_2 UVA-sol. All measurements were performed at 298 K. The titration solutions ([**L1**] $= 1.0 \times 10^{-5}$ M) were prepared by appropriate

(5) (a) van Asselt, R.; Elsevier, C. J. *J. Mol. Catal.* **1991**, *65*, L13. (b) van Asselt, R.; Elsevier, C. J. *Organometallics* **1992**, *11*, 1999.
(6) van Laren, W.; Elsevier, C. J. *Angew. Chem., Int. Ed.* **1999**, *38*, 3715–3717.
(7) Rieger, B.; Saunders Baugh, L.; Kacker, S.; Striegler, S. *Late Transition Metal Polymerization Catalysis*; Wiley-VCH: Weinheim, Germany, 2003.
(8) (a) Ittel, S. D.; Johnson, L. K.; Brookhart, M. *Chem. Rev.* **2000**, *100*, 1169. (b) Britovsek, G. J. P.; Gibson, V. C.; Wass, D. F. *Angew. Chem., Int. Ed.* **1999**, *38*, 429. (c) Gibson, V. C.; Spitzmesser, S. K. *Chem. Rev.* **2003**, *103*, 283.
(9) Groen, J. H.; Delis, J. G. P.; van Leeuwen, P. W. N. M.; Vrieze, K. *Organometallics* **1997**, *16*, 68.
(10) Durand, J.; Milani, B. *Coord. Chem. Rev.* **2006**, *250*, 542–560.
(11) Scarel, A.; Axet, M. R.; Amoroso, F.; Ragaini, F.; Elsevier, C. J.; Holuigue, A.; Carfagna, C.; Mosca, L.; Milani, B. *Organometallics* **2008**, *27*, 1486–1494.
(12) Small, B. L.; Rios, R.; Fernandez, E. R.; Carney, M. J. *Organometallics* **2007**, *26*, 1744–1749.
(13) (a) Gasperini, M.; Ragaini, F. *Organometallics* **2004**, *23*, 995. (b) Gasperini, M.; Ragaini, F.; Gazzola, E.; Caselli, A.; Macchi, P. *Dalton Trans.* **2004**, 3376. (c) Gasperini, M.; Ragaini, F.; Cenini, S. *Organometallics* **2002**, *21*, 2950–2957.
(14) (a) Fedushkin, I. L.; Khvoinova, N. M.; Baurin, A. Y.; Fukin, G. K.; Cherkasov, V. K.; Bubnov, M. P. *Inorg. Chem.* **2004**, *43*, 7807–7915. (b) Fedushkin, I. L.; Chudakova, V. A.; Skatova, A. A.; Khvoinova, N. M.; Kurskii, Y. A.; Glukhova, T. A.; Fukin, G. K.; Dechert, S.; Hummert, M.; Schummann, H. *Z. Anorg. Allg. Chem.* **2004**, *630*, 501–507. (c) Fedushkin, I. L.; Skatova, A. A.; Chudakova, V. A.; Khvoinova, N. M.; Baurin, A. Y.; Dechert, S.; Hummert, M.; Shumann, H. *Organometallics* **2004**, *23*, 3714–3718.
(15) *SMART* (control); *SAINT* (integration); Bruker Analytical X-Ray Systems: Madison, WI, 1994.
(16) Sheldrick, G. M. *SADABS, Program for Empirical Absorption Correction of Area Detector Data*; University of Göttingen: Göttingen, Germany, 1996.
(17) Sheldrick, G. M. *SHELXL-97, Program for the Refinement of Crystal Structures from X-Ray Data*; University of Göttingen: Göttingen, Germany, 1997.
(18) Spek, A. L. *PLATON, A Multipurpose Crystallographic Tool*; Utrecht University: The Netherlands, 2004.
(19) *MERCURY 1.4.1, Software for Visualising Crystal Structures*; The Cambridge Crystallographic Data Centre: Cambridge, U.K., 2005.

Table 1. Crystal and Structure Refinement Data for **L1** and **2**

	L1	**2**
empirical formula	$C_{32}H_{20}N_2$	$C_{32}H_{20}Cl_2N_2Pd$
fw	432.50	609.80
cryst syst; space group	monoclinic; $P2_1/c$	monoclinic; $P2_1/c$
unit cell dimensions (Å, deg)	$a = 11.349(2)$	$a = 11.810(4)$
	$b = 15.356(3)$	$b = 11.816(4)$
	$c = 13.820(3)$	$c = 18.125(6)$
	$\beta = 109.032(4)$	$\beta = 95.041(6)$
vol (Å^3)	2276.8(8)	2519.6(15)
Z; ρ_{calc} (g cm^{-3})	4; 1.262	4; 1.608
F(000)	904	1224
cryst size (mm^3)	0.49 × 0.40 × 0.18	0.24 × 0.19 × 0.07
abs coeff (mm^{-1})	0.074	0.974
θ range (deg)	1.90−28.01	1.73−27.98
max./min.transmission		1.000/0.759
reflns collected	10513	13536
independent reflns (R_{int})	4531 (0.0477)	5651 (0.0990)
final R indices [I > 2σ(I)]	R1 = 0.0623	R1 = 0.0943
	wR2 = 0.1476	wR2 = 0.1372

dilution of the stock solutions. Titrations of the ligand were carried out by the addition of microliter amounts of standard solutions of the ions in dichloromethane.

Mass Spectrometry. MALDI-TOF-MS analyses were obtained through the REQUIMTE-MALDI-TOF-MS Service Laboratory and were performed in a MALDI-TOF-MS voyager DE-PRO Biospectrometry Workstation equipped with a nitrogen laser radiating at 337 nm from Applied Biosystems (Foster City, CA). MALDI mass spectra were acquired and treated with the Data Explorer software, version 4 series. The MALDI-TOF-MS study in dichloromethane was carried out for **L** and **L1**, and for the Zn(II) and Pd(II) complexes **1** and **2**. Samples were dissolved in dichloromethane (1 μg/μL), and 1−2 μL of the corresponding solution was spotted on a well of a MALDI-TOF-MS sample plate and allowed to dry. No matrix was added. Measurements were performed in the reflector positive or negative ion mode, with a 20 kV accelerating voltage, 80% grid voltage, 0.005% guide wire, and a delay time of 200 ns. Mass spectral analysis for each sample was based on the average of 500 laser shots. TOF-MS-EI (time-of-flight mass spectrometry electron impact) and TOF-MS-FD (time-of-flight mass spectrometry field desorption) spectra were obtained at the REQUIMTE-MS Service Laboratory using a Micromass GCT model.

Computational Details. Unrestricted calculations were carried out using the Gaussian 03 package.[20] The hybrid density function method known as B3LYP was applied.[21] Effective core potentials were used to represent the innermost electrons of the transition atoms and the basis set of valence double-ζ quality for those associated with the pseudopotentials known as LANL2DZ.[22] A similar description was used for heavy elements such as chlorine and germanium, supplemented with an extra *d*-polarization function.[23] The basis set for the light elements such as C, N, and H was 6-31G*.[24] The structural data were obtained through a systematic search in the Cambridge Structural Database (version 5.28).[25]

Mono(1-naphthylimino)acenaphthene (L). 1-Aminonaphtalene (0.8 g, 5.4 mmol) in methanol (10 mL) was slowly added to a solution of acenaphthenequinone (1 g, 5.4 mmol) in methanol (100 mL) in the presence of formic acid (1 mL). After 15 min, a red precipitate was formed. The mixture was left stirring overnight at room temperature. After that, water was added (25 mL) to the reaction mixture, and the desired product was extracted with dichloromethane (3 × 15 mL). The organic layer (CH_2Cl_2) was separated and dried with $MgSO_4$ and filtered, and the solvent was removed with a rotary evaporator until dry. The solid residue was washed with diethyl ether (2 × 5 mL) and petroleum ether (3 × 10 mL), giving 1.54 g of pure product. Yield: 92%. Red crystals were obtained by recrystalization from a saturated dichloromethane hot solution. Anal. calcd (%) for $C_{22}H_{13}NO$ (M = 307.34): C, 85.97; H, 4.26; N, 4.56. Found: C, 85.63; H, 4.29; N, 4.54. ^{1}H NMR (400 MHz, CD_2Cl_2, 293 K): 8.21−8.18t (2H, Ar); 7.99−7.95t (2H, Ar); 7.91−7.81m (3H, Ar); 7.58−7.52m (2H, Ar); 7.42−7.39t (1H, Ar); 7.32−7.28t (1H, Ar); 7.12−7.10d (1H, Ar, J = 7.11 Hz); 6.77−6.75d (1H, Ar, J = 7.11 Hz). ^{13}C NMR (400 MHz, CD_2Cl_2, 293 K): 189.9 (C═O); 161 (C═N); 147.9 (C−N); 144.2; 134.9; 133.3; 131.8; 130; 128.8; 127.5; 125.8; 124.1; 122.6; 120.2; 112.6. IR Nujol (cm^{-1}): ν(C═O) 1724, ν(C═N) 1652. ESI: m/z 308.1 [**L** + H]$^+$; 330.1 [**L** + Na]$^+$.

Bis(1-naphthylimino)acenaphthene Zinc Dichloride (1). The bis(1-naphthylimino)acenaphthene zinc dichloride complex was prepared in a manner similar to that reported in the literature.[4] A suspension of acenaphthenequinone (2 g, 11 mmol) and $ZnCl_2$ (1.71 g, 12.5 mmol) was prepared in glacial acetic acid (15 mL). The 1-aminonaphtalene (3.6 g, 25 mmol) was added, and the reaction mixture was refluxed under stirring for 30 min. Then, it was allowed to cool down to room temperature, and a purple solid precipitated. The solid was separated by filtration and washed with cold acetic acid (2 × 10 mL). Then, it was washed with diethyl ether (5 × 10 mL), to remove all of the remaining acetic acid, and dried under a vacuum, giving 5.2 g of analytically pure purple product. Yield: 83%. Anal. calcd (%) for $C_{32}H_{20}Cl_2N_2Zn$ (M = 568.81): C, 67.57; H, 3.54; N, 4.92. Found: C, 66.94; H, 3.59; N, 4.74. ^{1}H NMR (400 MHz, CD_2Cl_2, 293 K): 8.16−8.14d (2H, Ar); 8.11−8.07m (6H, Ar); 7.76−7.54m (8H, Ar); 7.43−7.39tt (2H, Ar); 6.80−6.78d (1H, Ar, J = 7.35 Hz); 6.71−6.69d (1H, Ar, J = 7.35 Hz). ^{13}C NMR (400 MHz, CD_2Cl_2, 293 K): 165.5 (C═N); 146 (C−N); 141.5; 135; 133.2; 131.5; 129.4; 129.2; 129; 127.9; 127.8; 127.4; 127.3; 126.6; 126.5; 125.9; 125.7; 125.6; 123.7; 123.6; 118.4; 118.2. IR Nujol (cm^{-1}): ν(C═N) 1660, 1630. MALDI-TOF-MS: 432.52 [**L1**]$^+$ 100%, 533.4 [ZnCl(**L1**)]$^+$ 28%, 928.3 [Zn(**L1**)$_2$]$^+$ 9%. ESI: m/z 433.2 [**L1** + H]$^+$; 455.2 [**L1** + Na]$^+$; 928.3 [Zn(**L1**)$_2$]$^+$.

Bis(1-naphthylimino)acenaphthene (L1). The procedure for the synthesis of **L1** was the same as that described in the literature.[13c] Bis(1-naphthylimino)acenaphthene zinc dichloride (2 g, 3.3 mmol) was suspended in dichloromethane (200 mL), and a solution of potassium oxalate (0.181 g, 10 mmol) in water (10 mL) was added. The reaction mixture was left under strong agitation for 5 min. A

(20) Frisch, M. J.; Trucks, G. W.; Schlegel, H. B.; Scuseria, G. E.; Robb, M. A.; Cheeseman, J. R.; Montgomery, J. A., Jr.; Vreven, T.; Kudin, K. N.; Burant, J. C.; Millam, J. M.; Iyengar, S. S.; Tomasi, J.; Barone, V.; Mennucci, B.; Cossi, M.; Scalmani, G.; Rega, N.; Petersson, G. A.; Nakatsuji, H.; Hada, M.; Ehara, M.; Toyota, K.; Fukuda, R.; Hasegawa, J.; Ishida, M.; Nakajima, T.; Honda, Y.; Kitao, O.; Nakai, H.; Klene, M.; Li, X.; Knox, J. E.; Hratchian, H. P.; Cross, J. B.; Adamo, C.; Jaramillo, J.; Gomperts, R.; Stratmann, R. E.; Yazyev, O.; Austin, A. J.; Cammi, R.; Pomelli, C.; Ochterski, J. W.; Ayala, P. Y.; Morokuma, K.; Voth, G. A.; Salvador, P.; Dannenberg, J. J.; Zakrzewski, V. G.; Dapprich, S.; Daniels, A. D.; Strain, M. C.; Farkas, O.; Malick, D. K.; Rabuck, A. D.; Raghavachari, K.; Foresman, J. B.; Ortiz, J. V.; Cui, Q.; Baboul, A. G.; Clifford, S.; Cioslowski, J.; Stefanov, B. B.; Liu, G.; Liashenko, A.; Piskorz, P.; Komaromi, I.; Martin, R. L.; Fox, D. J.; Keith, T.; Al-Laham, M. A.; Peng, C. Y.; Nanayakkara, A.; Challacombe, M.; Gill, P. M. W.; Johnson, B.; Chen, W.; Wong, M. W.; Gonzalez, C.; Pople, J. A. *Gaussian 03*, revision C.2; Gaussian, Inc.: Wallingford, CT, 2004.

(21) (a) Becke, A. D. *J. Chem. Phys.* **1993**, *98*, 5648. (b) Lee, C.; Yang, W.; Parr, R. G. *Phys. Rev. B: Condens. Matter Mater. Phys.* **1988**, *37*, 785.

(22) Hay, P. J.; Wadt, W. R. *J. Chem. Phys.* **1985**, *82*, 299.

(23) (a) Hay, P. J.; Wadt, W. R. *J. Chem. Phys.* **1985**, *82*, 270. (b) Höllwarth, A.; Böhme, M.; Dapprich, S.; Ehlers, A. W.; Gobbi, A.; Jonas, V.; Köhler, K. F.; Stegman, R.; Veldkamp, A.; Frenking, G. *Chem. Phys. Lett.* **1993**, *208*, 237.

Scheme 1. Synthesis of Ligands **L** and **L1**[a]

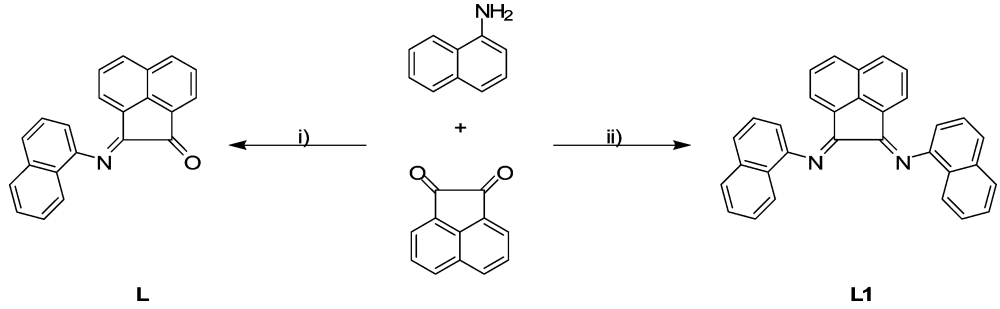

[a] (i) Ethanol/formic acid. (ii) 1-$ZnCl_2$/acetic acid, 2-potassium oxalate.

white precipitate of $Zn(C_2O_4)$ was present, suspended in the aqueous phase. The two phases were separated, and the organic layer was washed with water (3 × 20 mL), dried with $MgSO_4$, and filtered, and the solvent was removed under a vacuum, affording a red solid (1.45 g). Yield of the crude product: 95%. The red solid was then dissolved in toluene and filtered. The toluene solution was concentrated and petroleum ether (b.p.: 110−130 °C) added; red crystals suitable for single-crystal X-ray diffraction were formed while standing at room temperature. Anal. calcd (%) for $C_{32}H_{20}N_2$ (M = 432.51): C, 88.86; H, 4.66; N, 6.48. Found: C, 88.19; H, 4.97 N, 6.40. ^{1}H NMR (400 MHz, CD_2Cl_2, 293 K): 8.06−8.04d (2H, Ar); 8.0−7.98d (2H, Ar); 7.86−7.82t (4H, Ar); 7.63−7.55m (4H, Ar); 7.48−7.44t (2H, Ar); 7.26−7.22t + d overlapped (4H, Ar); 6.68−6.66d (2H, Ar, J = 7.29 Hz). ^{13}C NMR (400 MHz, CD_2Cl_2, 293 K): 162.4 (C═N); 148.9 (C−N); 142.3; 135; 131.7; 129.6; 128.6; 128.2; 127.2; 126.7; 126.3; 125.5; 125; 124.2; 124.0; 120.5; 112.7. IR Nujol (cm^{-1}): ν(C═N) 1661, ν(C═N) 1628. MALDI-TOF-MS: 432.6 [**L1**]$^+$ 100%, 864.5 [2**L1**]$^+$ 9%. ESI: *m*/*z* 455.2 [**L1** + Na]$^+$.

Bis(1-naphthylimino)acenaphthene Palladium Dichloride (2). Method A. A suspension of acenaphthenequinone (0.21 g, 1.12 mmol) and $PdCl_2$ (0.2 g, 1.12 mmol) was prepared in glacial acetic acid (15 mL). 1-Aminonaphtalene (0.32 g, 2.26 mmol) was added, and the reaction mixture was refluxed under stirring for 30 min. Then, it was left to cool down to room temperature, and a red-orange solid precipitated. The solid was separated by filtration and washed with cold acetic acid (2 × 10 mL). Then, it was washed with diethyl ether (5 × 10 mL), to remove all of the remaining acetic acid. The dark red solid was dissolved in a minimum amount of CH_2Cl_2 and filtered, and a black powder ("black palladium") was left undissolved. The CH_2Cl_2 solution was concentrated by removal of the solvent under a vacuum. Hexane was added and the solution left in the refrigerator. After 1 day, red crystals suitable for single-crystal X-ray diffraction were formed. Yield 50%. Anal. calcd (%) for $C_{32}H_{20}Cl_2N_2Pd$, (M = 609.84): C, 63.02; H, 3.31; N, 4.59. Found: C, 62.69; H, 3.84; N, 4.34. ^{1}H NMR (400 MHz, CD_2Cl_2, 293 K): 8.42−8.37m (2H, Ar); 8.14−8.12d (2H, Ar); 8.09−8.06t (4H, Ar); 7.76−7.62m (8H, Ar); 7.37−7.32tt (2H, Ar); 6.46−6.44d (1H, Ar); 6.41−6.39d (1H, Ar). ^{13}C NMR (400 MHz, CD_2Cl_2, 293 K): 177.3 (C═N); 148.2 (C−N); 142.5; 134.6; 133.2; 131.9; 129.9; 129.8; 129.6; 129.1; 127.9; 126.8; 125.9; 125; 123.5; 119.8. IR Nujol (cm^{-1}): ν(C═N) 1618. MALDI-TOF-MS: 432.6 [L1]$^+$ 100%, 465.6 [$C_{24}H_{16}N_4Pd$]$^+$ 25%; 499.6 [$C_{24}H_{16}ClN_4Pd$]$^+$ 7.4%, 537.5 [Pd(**L1**)]$^+$ 4%. ESI: *m*/*z*: 432.2 [L1]$^+$; 610.03 [$PdCl_2$(**L1**)+H]$^+$.

Method B. A suspension of $PdCl_2$, 0.3 g (1.69 mmol) in 50 mL of dry acetonitrile, was warmed to 70 °C in an argon atmosphere, to give a red solution. Then, a solution of 0.73 g of **L1** (1.69 mmol) in acetonitrile (20 mL) was added via cannula and the mixture refluxed for 1 h. A red solid precipitated. After that, the mixture was cooled to 20 °C, and the solvent was partially removed, and diethyl ether (20 mL) was added to complete precipitation. The solid product was separated by filtration and washed with diethyl ether (2 × 20 mL). It was recrystallized from dichloromethane/hexane (0.92 g). Yield 89%. Anal. calcd (%) for $C_{32}H_{20}Cl_2N_2Pd$, (M = 609.84): C, 63.02; H, 3.31; N, 4.59. Found: C, 62.87; H, 3.36; N, 4.58. ^{1}H NMR (600 MHz, CH_2Cl_2 293 K): 8.42−8.37m (2H, Ar); 8.14−8.12d (2H, Ar); 8.09−8.06t (4H, Ar); 7.76−7.62m (8H, Ar); 7.37−7.32tt (2H, Ar); 6.46−6.44d (1H, Ar); 6.41−6.39d (1H, Ar). ^{13}C NMR (600 MHz, CH_2Cl_2 293 K): 177.4 (C═N); 148.3 (C−N); 142.5; 134.6; 133.2; 131.9; 129.8; 129.6; 129.2; 127.9; 126.8; 125.9; 124.9; 123.5; 119.8. IR Nujol (cm^{-1}): ν(C═N) 1619. MALDI-TOF-MS: 432.6 [**L1**]$^+$ 100%, 465.6 [$C_{24}H_{16}N_4Pd$]$^+$ 16%; 499.6 [$C_{24}H_{16}ClN_4Pd$]$^+$ 3.52%, 537.5 [Pd(**L1**)]$^+$ 1%.

Results and Discussion

Synthesis and Characterization. Attempts to obtain **L1** by direct reaction of 1-aminonaphtalene with acenaphthenequinone in methanol in the presence of formic acid gives mono(1-naphthylimino)acenaphthene (**L**), independently of the stoichiometry (1:1 or 2:1), as red crystals in an almost quantitative yield (Scheme 1). The single-crystal X-ray structure of this compound was recently reported,[26] but the full characterization has not been reported; therefore, we have included it, in order to compare it with the bis(1-naphthylimino)acenaphthene, **L1**.

To be able to obtain bis(1-naphthylimino)acenaphthene, **L1**, the following method was adopted: first, bis(1-naphthylimino)acenaphthene zinc dichloride complex **1** was prepared in a manner similar to that reported in the literature[4] in 83% yield, by the reaction of 1-aminonaphtalene and acenaphthenequinone in a 2:1 stoichiometry, using the "template method", in the presence of $ZnCl_2$.

Second, subsequent demetalation of the ligand was obtained by treating a CH_2Cl_2 solution of [$ZnCl_2$(**L1**)] with an aqueous solution of potassium oxalate, leading to free **L1** in almost quantitative yield. It was then recrystallized from toluene/petroleum ether to yield red crystals, suitable for X-ray diffraction structure determination. The molecular structure of **L1** will be discussed below.

The complex bis(1-naphthylimino)acenaphthene palladium dichloride, **2**, was obtained by two different synthetic methods (A and B). In method A, compound **2** was obtained in a manner similar to that of the zinc complex, using the "template effect", at a 50% yield. The presence of "black

palladium" in the reaction due to metallic reduction can explain this low yield. To try to improve this yield, a second route was performed. Activation of $PdCl_2$, by refluxing it in acetonitrile, to give complex $[PdCl_2(NCCH_3)_2]$, as a non-isolated intermediate, followed by the addition of **L1**, gave **2** in 89% yield. We could grow red-orange single crystals of the anti isomer of **2** from CH_2Cl_2/hexane from the crude of the reaction of method A, and the solid-state structure was determined by X-ray diffraction. The molecular structure of **2** is discussed in the crystallographic section.

The FTIR spectrum of **L1**, recorded in Nujol, shows bands assigned to C═N stretching vibrations in the region ν = 1661−1628 cm^{-1}, while the IR spectrum of **L** shows frequencies at 1725 and 1652 cm^{-1} corresponding to C═O and C═N stretching vibrations, respectively. In the case of the metal complexes, the FTIR spectra display medium absorption bands in the region ν = 1660−1619 cm^{-1}, assigned to ν(C═N). The bands in the complexes are shifted to lower wave numbers, with respect to the free ligand, which is a criterion of the coordination of both diimine nitrogen atoms of the α-diimine ligands to the metallic ion. Selected IR absorption bands are listed in the experimental part. In the free ligand **L1** and in its metallic complexes, syn and anti isomers are possible. The syn and anti isomers are formed due to the different orientation of the naphthyl−N═C units: the chiral anti conformation having the two 1-naphthyl groups on different sides of the acenaphthenequinone plane, and the achiral syn conformation on the same side.

The free ligands **L** and **L1** and the metallic complexes of **L1** (**1** and **2**) were studied by ^{1}H, ^{13}C, and ^{1}H−^{1}H COSY; ^{1}H−^{13}C HSQC; ^{1}H−^{13}C HSQC-TOCSY; and ^{1}H−^{1}H NOESY NMR spectroscopies. All of the recorded spectra are included in the Supporting Information, Figures S1−S12. A comparison of the ^{13}C NMR spectra of **L** and **L1** shows differences, since **L** shows a peak at δ 189.9 ppm (C═O), which is not present in the ^{13}C NMR spectrum of **L1**. Inspection in detail of the ^{1}H and ^{13}C NMR spectrum at 293 K of **L1** in CD_2Cl_2 solution, see Figure S3 (Supporting Information), shows that only a set of signals are present, indicating that the syn and anti conformers are in fast exchange at that temperature on the NMR time scale. The variable-temperature ^{1}H NMR spectrum of **L1** was done at temperatures from 223 to 298 K, at 400 MHz in CD_2Cl_2, and it is shown in the Supporting Information, Figure S13. The most important changes observed are in the region from 8.1 to 7.9 ppm, where two doublets are transformed into a triplet, and in the region from 6.8 to 6.6 ppm, where a doublet shifts to a higher field. The transformation of the two doublets into a triplet can be explained by their overlapping. These signals shifting is a fact normally encountered by lowering the temperature of the NMR sample solution. No further splitting was found; therefore, interconversion between the syn and anti isomers takes place at this temperature range.

By comparison of the ^{1}H NMR spectra of the metallic complexes **1** and **2** synthesized by the "template method" with that of **L1** (Figure S14), we can see a duplication of the signals, indicating the presence of two isomers syn and anti in a 1:1 ratio. In the case of palladium complex **2**, the ^{1}H NMR spectra of the crude products obtained by methods A and B are different. The differences can be attributed to the existence of both isomers syn and anti in solution in a different proportion. In fact, the spectra are identical in the chemical shifts but different in the relative integration of the peaks. This is more apparent in the regions 7.4−7.3 ppm and 6.5−6.3 ppm, where we can see two superposed triplets and two doublets, respectively. In Figure S15 is shown the amplified 7.5−6 ppm region of compounds **1** and **2** (obtained by methods A and B).

Only the selected peaks in Figure S15 are assigned unequivocally. The doublets in the region of 6.5−6.3 ppm can be assign to the H(1,6), and the triplets in the region 7.4−7.3 ppm can be assigned to the H(2,5) of the acenaphthene ring, by ^{1}H,^{13}C,^{1}H,^{1}H COSY; ^{1}H,^{13}C HSQC; ^{1}H,^{13}C HSQC-TOCSY; and ^{1}H,^{1}H NOESY NMR experiments.

We can see therefore that, in the crude of **2** obtained by the "template method" (method A), the doublets showed equal intensity, whereas when the product was obtained by the activation of the palladium chloride and further reaction with **L1** (method B), the ratio in the intensities was different and equal to 1:3. That can be interpreted considering that in both reactions we get a mixture of both possible isomers syn and anti at a different rate; in the "template method", the probability of forming the isomer syn or anti is the same, as in the case of the complex **1** (ratio 1:1); when the reaction is done with method B, one orientation seems to be favored over the other, giving one of the isomers in a higher proportion (1:3). Once the isomers are formed, there is no interconversion in solution, as is discussed in the performed theoretical calculations.

Crystal Structures Description. The molecular structures of **L1** and **2** and the associated atom-numbering schemes are depicted in Figures 1 and 2, respectively. The free bis(1-naphthylimino)acenaphthene ligand (**L1**) exhibits (*E*,*Z*) isomeric preference instead of the common (*E*,*E*) pattern in the crystalline state, like other α-diimine compounds.[27] The different configurations of the imino units do not lead to important differences in the bond lengths [C1−N1 1.270(3), N1−C101 1.419(3), C11−N2 1.264(3), N2−C201 1.440(3) Å], being similar to those in related α-diimines.[27,28] The naphthalene moieties are almost perpendicular to each other, the value of the dihedral angle being 88.31(6)°. Concerning the arrangement of the naphthalene moieties in relation to

(24) (a) Hariharan, P. C.; Pople, J. A. *Theor. Chim. Acta* **1973**, *28*, 213. (b) Francl, M. M.; Petro, W. J.; Hehre, W. J.; Binkley, J. S.; Gordon, M. S.; DeFrees, D. J.; Pople, J. A. *J. Chem. Phys.* **1982**, *77*, 3654.
(25) Allen, F. H.; Kennard, O. *Chem. Des. Autom. News* **1993**, *8*, 31.
(26) Silvino, A. C.; Ferreira, L. C.; Dias, M. L.; Filgueiras, C. A. L.; Ḧ; orner, M.; Visentin, L.d C.; Bordinhao, J. *Acta Crystallogr., Sect E.* **2007**, *E63*, o999−o1000.
(27) (a) Amii, H.; Kohda, M.; Katagiri, T.; Uneyama, K. *J. Flourine Chem.* **2006**, *127*, 505–509. (b) Moore, J. A.; Vasudevam, K.; Hill, N. J.; Reeske, G.; Cowley, A. H. *Chem. Comm.* **2006**, 2913–2915. (c) See ref 14b.
(28) (a) Coventry, D. N.; Batsanov, A. S.; Goeta, A. E.; Howard, J. A. K.; Marder, T. B. *Polyhedron* **2004**, *23*, 2789–2795. (b) Cope-Eatough, E. K.; Mair, F. S.; Pritchard, R. G.; Warren, J. E.; Woobs, R. J. *Polyhedron* **2003**, *22*, 1447–1454.

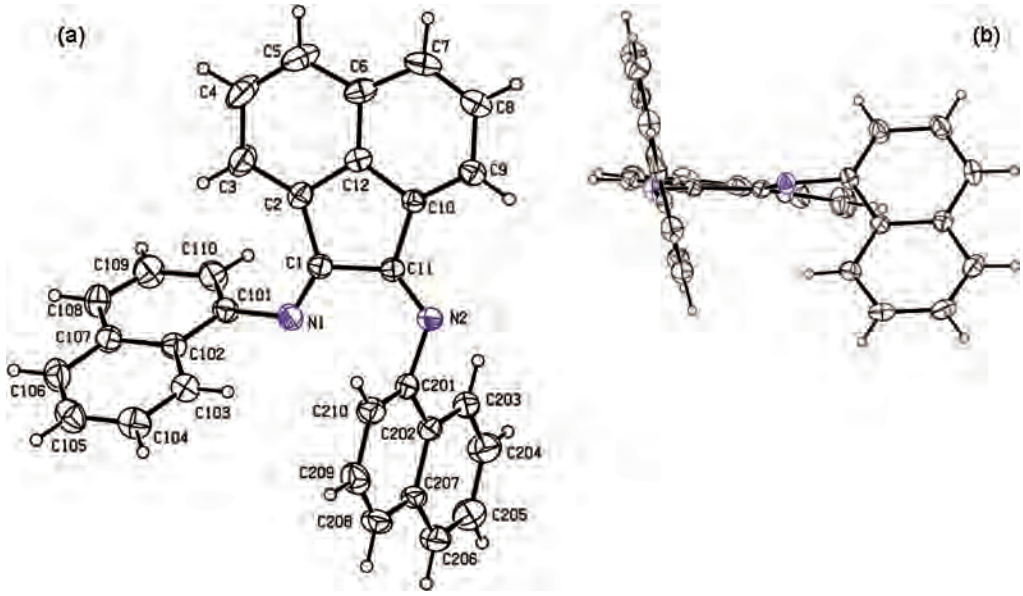

Figure 1. Displacement ellipsoid representations at the 30% probability level of **L1** (a) perpendicular and (b) parallel to the bis(imino)acenaphthene unit.

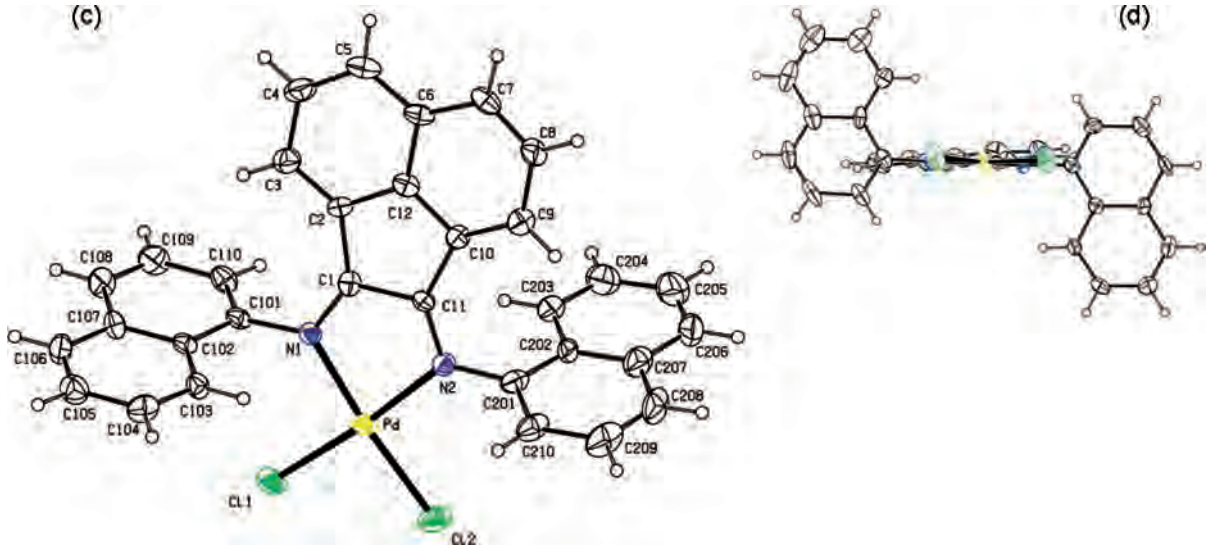

Figure 2. Displacement ellipsoid representation at the 30% probability level of **2** (c) perpendicular and (d) parallel to the bis(imino)acenaphthene unit. Selected bond lengths (Å) and angles (deg) for **2**: Pd−N1, 2.040(6); Pd−N2, 2.050(6); Pd−Cl2, 2.273(2); Pd−Cl1, 2.278(2); N1−Pd−N2, 81.4(2); N1−Pd−Cl2, 174.59(18); N2−Pd−Cl2, 93.30(19); N1−Pd−Cl1, 93.51(18); N2−Pd−Cl1, 174.60(19); Cl2−Pd−Cl1, 91.75(9).

the bis(imino)acenaphthene skeleton, the ligand shows anti orientation, and the dihedral angles between the naphthalene planes and the bis(imino)acenaphthene are 57.82(5)° (*Z* imine naphthalene) and 71.45(5)° (*E* imine naphthalene).

The coordination at the palladium in **2** is quite distorted from a regular square plane, where the relatively small N1−Pd−N2 bond angle of 81.4(2)° is a result of chelating ligand steric constraints. The bond angles and distances in the Pd(II) coordination plane (Figure 2) are very similar to the found values in other α-diimine−$PdCl_2$ complexes.[28,29] Comparison with the structural data of the free bis(1-naphthylimino)acenaphthene (**L1**; Figure 1) reveals some slight changes in the ligand which must be ascribed to the combined effects of changing the aromatic group on the imine N atoms and coordination to the palladium center. The imine C=N bonds C1−N1 and C11−N2 at 1.283(8) and 1.295(9) Å, respectively, are slightly longer than in the free ligand. Furthermore, upon coordination, the distance between the imine C atoms C1−C11 has decreased [1.531(3) Å in **L1** to 1.492(10) Å in **2**], and the diimine plane is more flat; the torsion angle N1−C1−C11−N2 is 10.4° in **L1** and 4.3° in **2**.[30] *E*,*Z* to *E*,*E* isomeric conversion of the α-diimine accompanies the coordination to the palladium atom. In this case, both naphthalene units, practically parallel to each other [dihedral angle of 6.72(21)°], are almost perpendicular to the bis(imino)acenaphthene plane [dihedral angles of 70.97(14) and 65.91(14)°] and also show anti orientation.

(29) (a) Camacho, D. H.; Salo, E. V.; Guan, Z.; Ziller, J. W. *Organometallics* **2005**, *24*, 4933–4939. (b) Schmid, M.; Eberhardt, R.; Klinga, M.; Leskela, M.; Rieger, B. *Organometallics* **2001**, *20*, 2321–2330.

(30) van Asselt, R.; Elsevier, C. J.; Smeets, W. J. J.; Spek, A. L. *Inorg. Chem.* **1994**, *33*, 1521–1531.

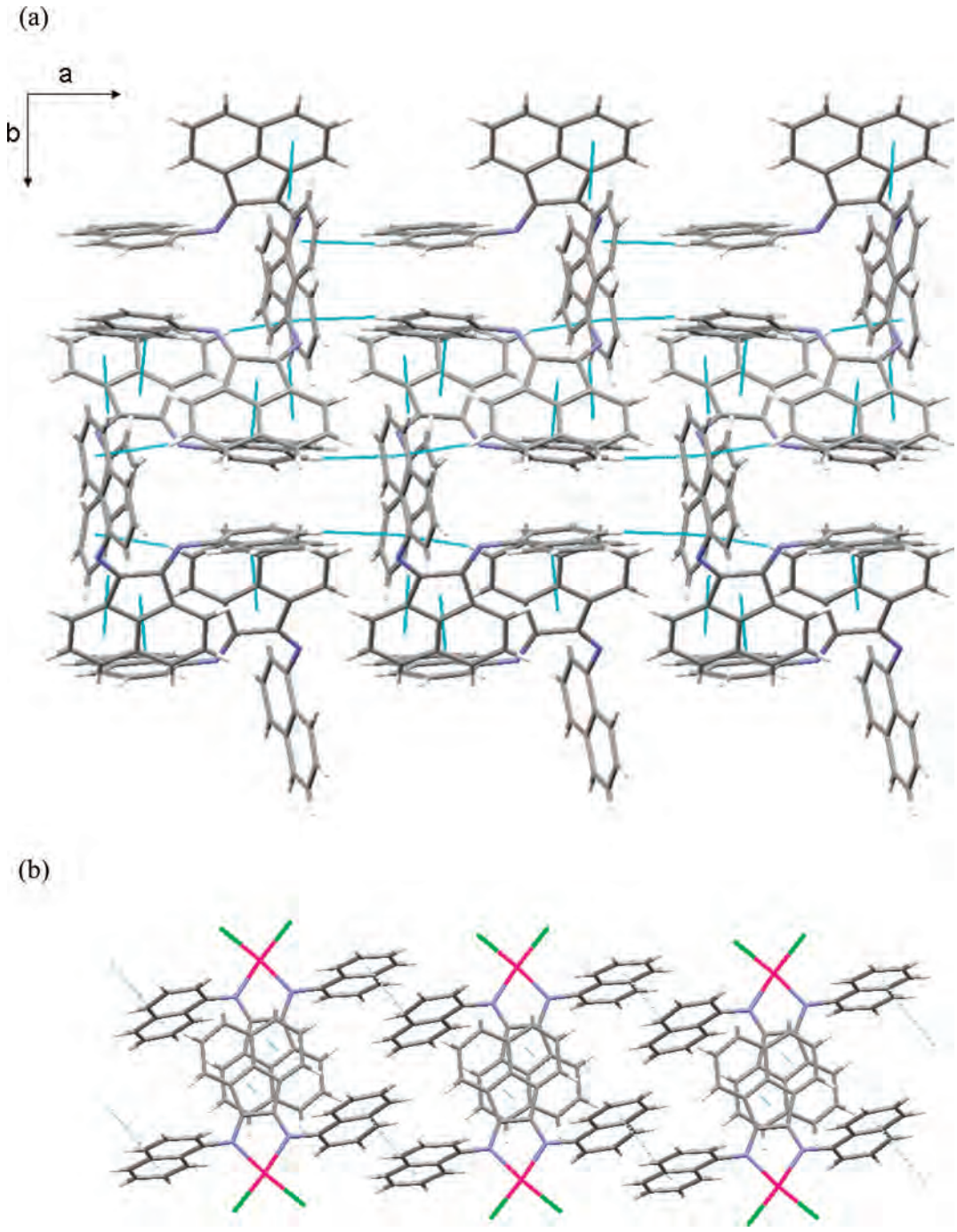

Figure 3. (a) Fragment of the infinite 3D network formed through C−H···π interactions among **L1** molecules, showing the packing in the *ab* plane. (b) Fragment of the infinite 1D ladderlike chain formed along of *a* axis through π···π interactions among molecules of **2**.

The nature of the ligand allows the formation of supramolecular architectures based on C−H···π[31] in **L1** and on π···π [32] interactions in **2**. Each **L1** molecule is joined to seven neighboring molecules through C−H···π interations [Cg(centroid)···H distance range 2.72−2.83 Å], generating a complicated 3D organization (Figure 3a). Supramolecular dimers of **2** are formed by π···π interactions involving the acenaphthene moieties ([C···C] = 3.547 Å, dihedral angle α: 2.56°). π···π interactions among the naphthalene units (d[C···C] = 3.400 Å, dihedral angle α: 6.75°) join the dimers, resulting in an infinite 1D ladderlike chain (Figure 3b).

Spectrophotometric Studies. Compound **L1** is provided by two conjugated imine functions but is remarkably different from others diimine compounds such as 2,2-bipyridine or 1,10-phenanthroline. In our case, the exocyclic nature of both imine bonds, out of the heteroaromatic ring systems, imposes better σ-donating and π-accepting properties as compared with bipyridine or phenanthroline.[33] This phenomenon modulated the photophysical properties of this type of compound.

The absorption spectra of **L1** in a CH_2Cl_2 solution at 298 K at concentrations between 1.0×10^{-6} and 1.0×10^{-4} M are reported in Figure S16A. Two well-defined bands are

Table 2. Optical Data for **L**, **L1**, and Its Zn(II) and Pd(II) Complexes in a Freshly Prepared Dichloromethane Solution at Room Temperature

	Absorption[a]
compounds	λ_{max}/ nm (10^{-3} ε, M^{-1} cm^{-1})
L	254 (37.5); 303 (19.3); 372*sh* (2.2); 457 (1.8)
L1	305 (42.3); 432 (5.2)
[$ZnCl_2$(**L1**)]	266 (426.4); 325*sh* (145.0); 468 (5.1)
[$PdCl_2$(**L1**)]	266 (478.6); 327 (373.7); 400*sh* (10.1); 542*sh* (1.7)

[a] In non degassed solutions. *sh* = shoulder.

observed in the spectrum. The first transition of compound **L1** appearing in the range $400 < \lambda < 550$ nm can be readily assigned to intraligand transitions of the free diimine compound, as previously reported for similar BIAN diimine ligands,[34] while the second one at $250 < \lambda < 350$ nm can be assigned to the naphthalene moiety.[35] The naphthalene absorption contribution is also observed in Figure S17 (Supporting Information), where the absorption spectra of both organic precursors of ligand **L1**, 1-naphthylamine and acenaphthenquinone, are represented. In both spectra, obtained in dichloromethane solution at 1.0×10^{-5}M at room temperature, the absorption band appears in the region $250 < \lambda < 350$ nm. The second band observed for ligand **L1** in the range $400 < \lambda < 550$ nm is also present, but with less intensity for the monoimine ligand **L** (Figure S17). The absence of bands in the infrared region of the absorption spectra of **L1** confirms that no anionic states due to reduction are present in this BIAN-derivate ligand.[36]

In Table 2 are summarized all optical data for ligands **L** and **L1** and for the Zn(II) and Pd(II) complexes of **L1**. Figure S16B shows the absorption spectra at different concentrations of complex **2** in fresh dichloromethane solution. Bands at 266, 327, 400*sh,* and 542*sh* nm are observed. The shoulder observed at 542 nm could be assigned to the metal-to-ligand charge-transfer transitions from the metal center to the π^* orbital of **L1**. The three previous bands at 266, 327, and 400 nm, present also in the free ligand, are red-shifted when compared with **L1** and could be assigned to the $\pi-\pi^*$ transitions in the naphthalene moieties (intraligand transitions) observed in the free diimine compound.

The stoichiometry of complex **2** was obtained from a metal titration experiment using a fresh dichloromethane solution. This experiment is shown in Figure S18. The band centered at 300 nm is 16-nm red-shifted after metal complexation. This effect confirms that metal complexation takes place. Detailed inspection of the inset in Figure S18 shows a plateau reached after the addition of an equivalent amount of Pd(II), which suggests that each **L1** unit is coordinated to one Pd(II) ion. This stoichiometry was confirmed in the solid state by the X-ray structure.

Both ligands **L** and **L1** are not luminescent in dichloromethane. The expected fluorescence emission of **L1** as a naphthalene derivative[35] is totally quenched, even when the ligand is complexed to Zn(II).[37] This behavior is probably due to the absence of any spacer between the emissive unit (naphthalene chromophore) and the chelation unit (imine nitrogen) that permits a fast electron transfer process from the lone pair of electrons present in the imine nitrogen atoms to the emissive naphthalene chromophores.[38]

Mass Spectrometry Studies. Both organic ligands, **L** and **L1**, and the Zn(II) and Pd(II) complexes of **L1** have been studied by mass spectrometric techniques: MALDI-TOF-MS, TOF-MS-EI, and TOF-MS-FD. Samples were dissolved in fresh dichloromethane (1 μg/μL), and 1−2 μL of the corresponding solution was spotted on a well of a MALDI-TOF-MS sample plate and allowed to dry. For TOF-MS-EI^+ and TOF-MS-FD^+, the sample was introduced directly.

In all MALDI-TOF-MS studies, no matrix was added, instead using the organic ligand as a new *in situ* MALDI-TOF-MS matrix.[39] In this case, the measurements were performed in the reflector positive or negative ion mode, with a 20 kV accelerating voltage, 80% grid voltage, 0.005% guide wire, and a delay time of 200 ns.

Figure S19 shows the TOF-MS-FD^+ spectrum of complex **2**. The spectrum shows peaks at 610.0 *m*/*z* assigned to the complex [$PdCl_2$(**L1**)]$^+$, and the fragmentations at 575.6, 538.0, and 433.1 *m*/*z* are assigned to the fragments [Pd-Cl(**L1**)]$^+$, [Pd(**L1**)]$^+$, and [**L1**]$^+$. In the high mass region, a peak corresponding to the dimeric species [Pd($\mathbf{L1}_2$)]$^+$ at 971.7 *m*/*z* also appears. Similar peaks and fragmentations have been observed by MALDI-TOF-MS spectrometry (see Figure S20).

The peak at 610.0 *m*/*z* assigned to the complex [$PdCl_2$-(**L1**)]$^+$ is shown in Figure S21 together with the isotopic theoretical model calculated with the software MASS LYNX by micromass, confirming our attribution.

In Figures S22 and S23 show the TOF-MS-EI and MALDI-TOF-MS spectra for ligands **L** and **L1**, respectively. In both cases, the molecular ion peaks at 307.09 *m*/*z* and 431.58 *m*/*z* assigned to [**L**+H]$^+$ and [**L1**+H]$^+$, respectively, are observed. Fragmentation peaks and peaks due to the formation of dimeric species for **L1** are also observed. Both spectra are very clear, suggesting the potential use of both organic compounds as MS matrices.

The MALDI-TOF-MS spectra of complex **1** are also shown in the Supporting Information (Figure S24). Peaks at 532.4 and 433.5 *m*/*z*, assigned to the fragments [ZnCl(**L1**)]$^+$

(31) Nishio, M. *CrystEngComm* **2004**, *6*, 130–158.
(32) Janiak, C. *J. Chem. Soc., Dalton Trans.* **2000**, 3885–3896.
(33) (a) Johnson, L. K.; Filian, C. M.; Brookhart, M. *J. Am. Chem. Soc.* **1995**, *117*, 6414–6415. (b) Reinhold, J.; Benedix, R.; Birner, P.; Henning, H. *Inorg. Chim. Acta* **1979**, *33*, 209–231.
(34) Paulovicova, A.; El-Ayaan, U.; Shibayama, K.; Morita, T.; Fukuda, Y. *Eur. J. Inorg. Chem.* **2001**, 2641–2646.
(35) (a) de Melo, J. S.; Alberta, M. T.; Díaz, P.; García-España, E.; Lodeiro, C.; Alves, S.; Lima, J. C.; Pina, F.; Soriano, C. *J. Chem. Soc., Perkin Trans. 2* **2002**, *5*, 991–998. (b) Pina, J.; de Melo, J. S.; Pina, F.; Lodeiro, C.; Lima, J. C.; Parola, A. J.; Soriano, C.; Clares, M. P.; Alberta, M. T.; Aucejo, R.; García-España, E. *Inorg. Chem.* **2005**, *44*, 7449–7458. (c) Aucejo, R.; Alarcón, J.; García-España, E.; Llinares, J. M.; Marchin, K. L.; Soriano, C.; Lodeiro, C.; Bernardo, M. A.; Pina, F.; Pina, J.; de Melo, J. S. *Eur. J. Inorg. Chem.* **2005**, 4301–4308.
(36) (a) Fedushkin, I. L.; Lukoyanov, A. N.; Ketkov, S. Y.; Hummert, M.; Schumann, H. *Chem.—Eur. J.* **2007**, *13*, 7050–7056. (b) Fedushkin, I. L.; Skatova, A. A.; Chudakova, V. A.; Cherkasov, V. K.; Fukin, G. K.; Lopatin, M. A. *Eur. J. Inorg. Chem.* **2004**, 388–393.
(37) (a) Bermejo, M. R.; Vazquez, M.; Sanmartin, J.; García-Deibe, A. M.; Lodeiro, C. *New J. Chem.* **2002**, *26*, 1365–1370. (b) Fondo, M.; García-Deibe, A. M.; Ocampo, N.; Sanmartin, J.; Bermejo, M. R.; Oliveira, E.; Lodeiro, C. *New J. Chem.* **2008**, *32*, 247–257.
(38) Pina, F.; Lima, J. C.; Lodeiro, C.; de Melo, J. S.; Díaz, P.; Albelda, M. T.; García-España, E. *J. Phys. Chem. A* **2002**, *106*, 8207–8212.

Scheme 2. NMR Numbering of the Compounds, R = O or N-naphthyl

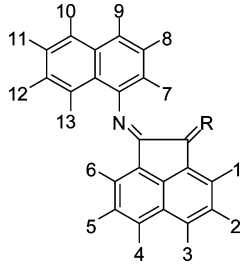

Scheme 3. Definition of Parameter τ to Describe the Relative Orientation between Acenaphthylene and Naphthyl Groups

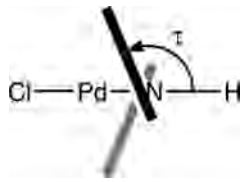

and $[\mathbf{L1}]^+$, are observed. A peak at 930.3 *m*/*z*, assigned to the dimeric complex $[Zn(\mathbf{L1})_2]^+$, is also observed.

Theoretical Study. Density functional calculations have been performed in order to determine the relative stability of each isomer of compound **2**. The optimized molecular geometry is very similar in both isomers, and only a few differences can be found. In general, distances are identical in both isomers (*i.e.*, Pd−N and Pd−Cl are 2.12 and 2.31 Å, respectively), and angles around the palladium atom change only 0.1°. More significant is the variation in the angle between acenaphthylene and naphthyl groups, defined by τ in Scheme 3 (104.4 and 99.8° for anti and syn, respectively).

The full optimization of molecular structure shows that the anti isomer is more stable than *syn*-[$PdCl_2$(BIAN)]. However, the difference of energy is only 0.07 kJ·mol^{-1}, and we consider both conformers as isoenergetic. Behind their similar stability, one can anticipate the possible formation of both complexes in solution. This result can be confirmed by a search of complexes having the BIAN ligand, [ML_n(BIAN)], in the Cambridge Structural Database, in which both isomers crystallize when the substituents are asymmetric: anti[40] or syn.[41]

Similarly to the complex [$PdCl_2$(BIAN)], free ligand BIAN can present anti and syn conformers, having the same relative stability (anti is the most stable by 0.06 kJ·mol^{-1}) and similar structural parameters (*i.e.*, $\tau \approx 125°$). The interconversion between both isomers can be possible by rotating a $N-C_{naphthyl}$ bond. Consequently, a transition state is located that has one coplanar naphthyl group to acenaphthylene rings (τ is 177 and 125° for each naphthyl group), and its energy, +18.7 kJ·mol^{-1}, is accessible at room temperature (Figure 4). However, when the $PdCl_2$ fragment is introduced into

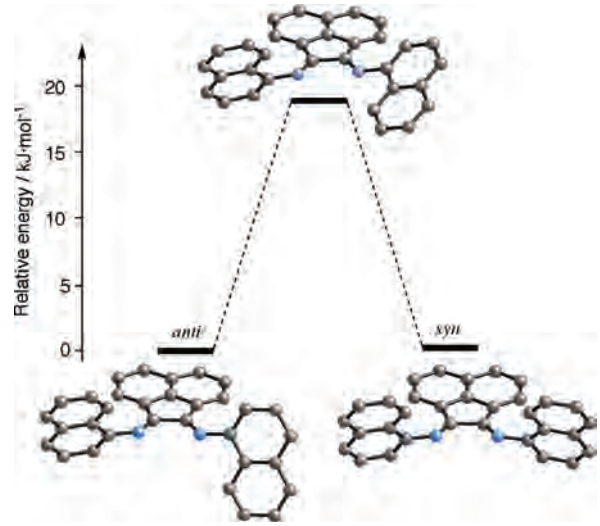

Figure 4. Energetic profile for the free BIAN ligand. Atomic coordinates are available from Table S2, Supporting Information.

the ligand, a corresponding transition state for the conversion between *anti*- and *syn*-[$PdCl_2$(BIAN)] is computably unavailable, probably due to the proximity of the naphthyl moiety to the chloride ligand in square-planar geometry. However, one cannot reject obtaining both isomers at different rates, by changing the experimental conditions as indicated above. In agreement, fluxionality has been detected by ^{1}H NMR spectroscopy in compounds having metallic fragments with less steric requirements, such as Ge (R = 2,6-diisopropylphenyl).[40a] Moreover, dynamic behavior in Mg or Ca complexes (R = 2,5-ditert-butylphenyl) having the terminal ligand perpendicular to the BIAN ligand has also been found.[40b]

To evaluate the possible conversion between anti and syn isomers, we have calculated the energy profile as a function of the torsion angle for the $N-C_{naphthyl}$ bond, τ_1. In these partial optimizations, only this torsion angle is kept constant for one bond, and all other geometric parameters have been relaxed, including the second $N-C_{naphthyl}$ bond, τ_2. As is found in full optimization, one minimum is found for each conformer (*ca.* ∼ 100°). When τ_1 angles are close to the transition state in the complex, for example, 160°, the molecular energy increases ∼40 kJ·mol^{-1} from the minimum in both conformations, and an estimation for coplanar rings ($\tau_1 = 180°$) could reach values near +80 kJ·mol^{-1}. In this case, the process is unfavored, and we will anticipate that this reaction does not occur. Finally, we notice that the inverse rotation by approaching a naphthyl moiety at acenaphthylene ($\tau = 0°$) is always higher in energy.

A second piece of information can be obtained from Figure 5 due to the smooth profile for both conformers. If a limit of 8 kJ·mol^{-1} is assumed for intermolecular packing forces, available values for τ would be between 50 and 130°. Consequently, a wide experimental range can be expected for τ, of 80°, in agreement with experimental data having values of 68 and 109° for **2**. However, in an attempt to compare our results with structural data, we found it impossible to define the relative orientation for the symmetric substituent in the *N*,*N*′-acenaphthylene ligand and differenti-

(39) Pedras, B.; Santos, H. M.; Fernándes, L.; Covelo, B.; Tamayo, A. M.; Bértolo, E.; Capelo, J. L.; Avilés, T.; Lodeiro, C. *Inorg. Chem. Commun.* **2007**, *8*, 925–929.

(40) (a) Ge: see ref 14c. (b) MgL_2: see ref 14b. (c) NiL_2: Gates, D. P.; Svejda, S. A.; Oñate, E.; Killian, C. M.; Johnson, L. K.; White, P. S.; Brookhart, M. *Macromolecules* **2000**, *33*, 2320. (d) $MNiL_2$: Cherian, A. E.; Rose, J. M.; Lobkovsky, E. B.; Coates, G. W. *J. Am. Chem. Soc.* **2005**, *127*, 13770. (e) NiL_4: see ref 40c.

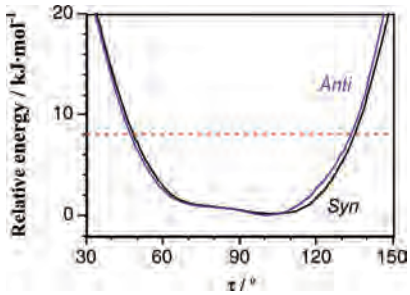

Figure 5. Energy as a function of the τ angle in both isomers of compound [$PdCl_2$(BIAN)]. Zero values for each conformer are taken arbitrary to the minimum.

ate τ, and its complementary $180 - \tau$ (there are not significant data for asymmetric substituents) reduces the range to 50−90°. In accordance, experimental data in the Cambridge Structural Database for related complexes show that most expected values are maxima between 70° and 90°, and the range decreases when only square-planar complexes are considered (75−85°, see Figure S25). Moreover, the variation of τ for one naphthyl group has little influence in the other group. The second naphthyl prefers angles of about 100 or 110°, except when τ is changed too. Experimental values show that differences between both substituents are normally less than 15° (Figure S26).

We continue searching other fragments ML_n attached to the BIAN ligand in order to compare the geometry and relative stability of both conformers for complexes [ML_n(BIAN)]. These fragments are neutral and have different geometries in order to estimate the importance of external ligands in the coordination sphere of metal. The studied cases are (*a*) Ge; (*b*) AuCl and CuCl; and (*c*) $NiCl_2$, $CoCl_2$, and $ZnCl_2$, for $n = 0$, 1, and 2, respectively. These results are shown in Table 3.

In general, differences in geometric parameters between isomers are less than 0.01 Å for distances and 0.3° for bond angles, and we can suppose that energetic differences are introduced only by the coordination of metallic fragment ML_n. The germanium compound has an important behavior with respect to transition metal complexes: the torsion angle τ is always less than 90° in both isomers. Only in this case, the syn conformer is more stable than the anti one, by only 0.3 kJ·mol^{-1}. We can confirm that the presence of Ge binding to N donors does not change the small differences between isomers.

A similar result has been obtained for [AuCl(BIAN)]. The gold atom presents a lineal coordination (N−Au−Cl ≈ 175°), being coplanar to the acenaphthylene ligand. The small influence due to the presence of the chloride ligand is reflected in the small energetic difference between both structures, although the anti form is in this case the most stable. This difference increases to 2 kJ·mol^{-1} for [CuCl(BIAN)], probably because of the different coordination number in the syn and anti isomers, having perfectly trigonal and intermediate geometries around the copper atom (Scheme 4a).

Calculations have also been performed for complexes of Zn(II), Co(II), and Ni(II) with a tetrahedral environment. Structures for $ZnCl_2$ and $CoCl_2$ can be considered analogues to the $PdCl_2$ square-planar complex, by changing the environment of the transition metal. The energetic difference is ∼ 3 kJ·mol^{-1}, where the anti conformer is stabilized by the best directionality of the hydrogen bonds such as (C)H···Cl(M)[42] (see Scheme 4b: H$^{(8)}$···Cl are ∼2.87 and 2.80 Å for Zn and Co). As a result, the MCl_2 fragments are perpendicular to BIAN for the syn conformer, but those are turned about 11° for the anti one (Scheme 4b).

A special mention is made for Ni(II), which can present two spinomers.[43] Six structures have been published having the BIAN ligand, and its coordination is essentially tetrahedral, and only one compound with a π-acid ligand such as allyl has a square-planar environment. Consequently, we have considered tetrahedral geometry for [$NiCl_2$(BIAN)], in which the relative energy decreases to 1.1 kJ·mol^{-1}. Since the anti form is analogous to that of Co and Zn complexes (H$^{(8)}$···Cl ≈ 2.73 Å), the syn one presents an asymmetric orientation for naphthyl groups (τ = 112 and 66°), being the only structure together with both of the Ge compounds having τ < 90°. The molecular geometry implies two different short contacts for each chlorine atom (H$^{(8)}$···Cl ≈ 2.77 and H$^{(2)}$···Cl′ ≈ 2.89 Å) and a deviation from perpendicularity of 4°. These distortions from idealized geometry, such as the Cl−Ni−Cl angle at about 143°, can be assigned to no spherical distribution of electronic density for a d^8 ion in a tetrahedral environment.[44]

Finally, any octahedral complexes were calculated; however, simple models suggest that conclusions obtained for square-planar ones can be applied to these compounds.

Conclusions

A new rigid bidentate ligand bis(1-naphthylimino)acenaphthene, **L1**, and its Zn(II) and Pd(II) complexes [$ZnCl_2$(**L1**)], **1**, and [$PdCl_2$(**L1**)], **2**, were synthesized. **L1** was prepared by the "template method", reacting 1-naphthyl amine and acenaphthenequinone in the presence of $ZnCl_2$, giving **1**, which was further demetallated. Reaction of 1-naphthyl amine with acenaphthenequinone and $PdCl_2$ afforded dichloride bis(1-naphthyl)acenaphthenequinonediimine) palladium, **2**. **L1**, **1**, and **2** were obtained as a mixture of syn and anti isomers. Compound **2** was also obtained by the reaction of $PdCl_2$, activated by refluxing it in acetonitrile, followed by the addition of **L1**; by this route, a mixture of syn and anti isomers was also obtained, but at a different rate. All compounds have been characterized by elemental analyses; MALDI-TOF-MS spectrometry; IR; UV−vis; ^{1}H, ^{13}C, ^{1}H−^{1}H COSY; ^{1}H−^{13}C HSQC; ^{1}H−^{13}C HSQC-TOCSY; and ^{1}H−^{1}H NOESY NMR spectroscopies when applied.

The solid-state structures of **L1** and the anti isomer of compound **2** have been determined by single-crystal X-ray diffraction. The coordination at the palladium in the anti isomer of compound **2** is quite distorted from an ideal square-

(41) (a) Ge: see ref 14c. (b) CaL_3: see ref. 14b. (c) NiL_3: Maldanis, R. J.; Wood, J. S.; Chandrasekaran, A.; Rausch, M. D.; Chien, J. C. W. *J. Organomet. Chem.* **2002**, *645*, 158.
(42) Aullón, G.; Bellamy, D.; Brammer, L.; Bruton, E. A.; Orpen, A. G. *Chem. Commun.* **1998**, 653.
(43) Cirera, J.; Ruiz, E.; Alvarez, S. *Inorg. Chem.* **2008**, *47*, 2871.
(44) Ruiz, E.; Cirera, J.; Alvarez, S. *Coord. Chem. Rev.* **2005**, *249*, 2649.

Table 3. Selected Structural Parameters for Optimized Complexes Having BIAN Ligand in Both Conformations[a]

ML_n	geometry	conformation	τ	M−N	M−Cl	N−M−N	N−M−Cl	Cl−M−Cl	ω[e]	energy[f]
	free ligand	anti	125.2							
		syn	124.7							+0.06
Ge	bent	anti	72.4	1.932						
		syn	71.1	1.932						−0.31
AuCl	linear[b]	anti	97.8	2.112	2.318	66.9	175.0			
		syn	95.8	2.110	2.318	66.9	174.9			+0.24
CuCl	trigonar[c]	anti	115.7, 130.3	2.004, 2.398	2.151	76.7	160.9, 122.3			
		syn	122.9	2.151	2.165	78.5	140.8			+2.15
$PdCl_2$	square-planar	anti	99.8	2.115	2.311	79.5	94.4	91.8	0.1	
		syn	104.4	2.117	2.312	79.4	94.5	91.6	3.8	+0.07
$ZnCl_2$	tetrahedral	anti	121.5	2.231	2.352	77.0	103.4, 112.5	133.9	79.1	
		syn	114.3	2.235	2.351	77.0	105.8, 110.0	133.8	90.0	+2.86
$NiCl_2$[d]	tetrahedral	anti	116.0	2.088	2.249	81.7	98.9, 109.1	142.9	79.1	
		syn	66.2, 112.1	2.077	2.248	81.8	102.6, 104.9	143.3	85.8	+1.14
$CoCl_2$	tetrahedral	anti	123.0	2.142	2.242	80.5	104.9, 114.9	127.1	78.9	
		syn	116.1	2.147	2.241	80.5	108.2, 111.8	126.8	89.5	+3.29

[a] Distances are in Ångstroms, angles in degrees, and energies kilojoules per mole. [b] Second *N* donor is not coordinated (N···Au not-bonded distances are 2.932 and 2.936 Å, respectively). [c] Coordination of BIAN for the anti isomer is asymmetric. [d] Syn isomer has two "different" orientations for naphthyl groups. [e] Angle ω is defined between BIAN and MCl_2 planes. [f] Positive values mean that the anti isomer must be the most stable.

Scheme 4. Molecular Diagram for Some Complexes $[ML_n(BIAN)]$ Discussed in the Text[a]

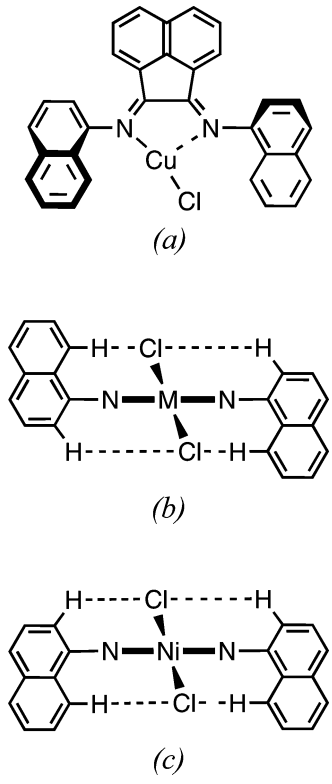

[a] (a) *anti*-[CuCl(BIAN)]; (b) *anti*-$[MCl_2(BIAN)]$ (M = Zn, Co, Ni); and (c) *syn*-$[NiCl_2(BIAN)]$.

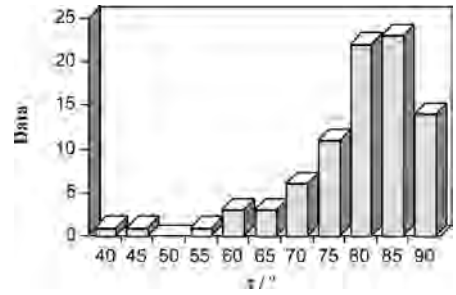

Figure 6. Experimental τ values in complexes $[ML_n(BIAN)]$ in crystal structures having an analogous ligand to BIAN. Data are retrieved for crystal structures from the Cambridge Structural Database.

plane environment, where the relatively small N1−Pd−N2 bond angle of 81.4(2)° is a result of chelating ligand steric constraints. Theoretical calculations show that the molecular geometry is very similar in both isomers, and only an important variation in the orientation angle for naphthyl groups can be expected, in agreement with the experimental structure. DFT studies showed that the syn and anti isomers of $[PdCl_2(BIAN)]$ are isoenergetics; therefore, they can both be obtained experimentally. However, no isomerization process is available in square-planar complexes, but it can occur for the free ligand. Finally, by replacing the metallic fragment ML_n, the structural choice can be affected, and one or both conformers can be obtained. Their relative stability will depend on the nature of the metal, including the electronic configuration and environment, and on the terminal ligands.

Acknowledgment. We thank Fundação para a Ciência e Tecnologia, Portugal, for funding (Projects PTDC/QUI/66440/2006, PTDC/QUI/66250/2006) and for a doctoral fellowship to V.R. (SFRH/BD/13777/2003). We also thank the Portuguese−Spanish Integrated Action-2008, No. E-77/08. Financial support for this work was also provided by the Spanish Dirección General de Investigación (DGI) through Grant CTQ2005-08123-C02-02/BQU and by the Departament d'Universitats, Recerca i Societat de la Informació (DURSI) of Generalitat de Catalunya through Grant 2005SGR-0036. The computing resources at the Centre de Supercomputació de Catalunya (CESCA) were made available in part through a grant of Fundació Catalana per a la Recerca (FCR) and Universitat de Barcelona.

Supporting Information Available: This material is available free of charge via the Internet at http://pubs.acs.org.

IC800790U